^{64}Cu-based Radiopharmaceuticals in Molecular Imaging

Yeye Zhou, MB[1]⑩, Jihui Li, MD[1], Xin Xu, MB[1], Man Zhao, MB[1], Bin Zhang, PhD[1], Shengming Deng, PhD[1], and Yiwei Wu, PhD[1]

Abstract

Copper-64 ($T_{1/2}$ = 12.7 hours; β^+: 19%, β^-: 38%) has a unique decay profile and can be used for positron emission tomography imaging and radionuclide therapy. The well-established coordination chemistry of copper allows for its reaction with different types of chelator systems. It can be linked to antibodies, proteins, peptides, and other biologically relevant small molecules. Two potential ways to produce copper-64 radioisotopes concern the use of the cyclotron or the reactor. This review summarized several commonly used biomarkers of copper-64 radionuclide.

Abbreviations

CT, computed tomography; PET, positron emission tomography; SPECT, single photon emission computed tomography; HNSCC, head and neck squamous cell carcinoma; Cu-ATSM, Cu-diacetyl-bis (N4-methylthiosemicarbazone); NSCLC, non-small cell lung cancer; HNC, head and neck cancer; SUV, standardized uptake value; HTV, hypoxic tumor volume; HB, hypoxic burden; FAS, fatty acid synthase; PCa, prostate cancer; MRI, magnetic resonance imaging; EFGR, epidermal growth factor receptor; HER2, Human epidermal growth factor receptor; IHC, immunohistochemistry; mAb, monoclonal antibodies; SCC, squamous cell carcinoma; OC, octreotide; NPV, negative predictive value; SOD, superoxide dismutase; uPA, urokinase-type plasminogen activator; uPAR, urokinase-type plasminogen activator receptor; PSMA, prostate-Specific Membrane Antigen

Introduction

As molecular imaging continues to advance, positron emission tomography (PET) and single photon emission computed tomography (SPECT) technology are nowadays an integral part of the molecular imaging toolbox. Dual-modality imaging, such as PET/computed tomography (CT) or SPECT/CT, integrates the high-resolution anatomical images with physiological information, which enables the investigators to identify the physiological basis of the disease and correlate it with the anatomical image.[1]

Radioactive copper is one of the most actively studied radionuclides.[2-4] Several reasons render this element so attractive for PET imaging. The long half-life of the copper allows sufficient uptake and distribution to yield considerable contrast and quality of images. In addition, copper can react with many chelator systems due to its well-established coordination chemistry, and it can be linked to antibodies, proteins, peptides,

and other biologically relevant small molecules.[5] The most extensively used class of chelators for ^{64}Cu has been shown in Figure 1. Among the 27 known copper radioisotopes, 5 of them are particularly interesting for molecular imaging applications (^{60}Cu, ^{61}Cu, ^{62}Cu, and ^{64}Cu) and in radiotherapy (^{64}Cu and ^{67}Cu).[4] Table 1 lists their nuclear characteristics.

Availability of Cu isotopes for preclinical and clinical research has been greatly improved in the recent years, since many potential chelators have been developed over the last

[1] Department of Nuclear Medicine, The First Affiliated Hospital of Soochow University, Suzhou, China

Corresponding Authors:
Shengming Deng, PhD, and Yiwei Wu, PhD, Department of Nuclear Medicine, The First Affiliated Hospital of Soochow University, Suzhou, 215000, China.
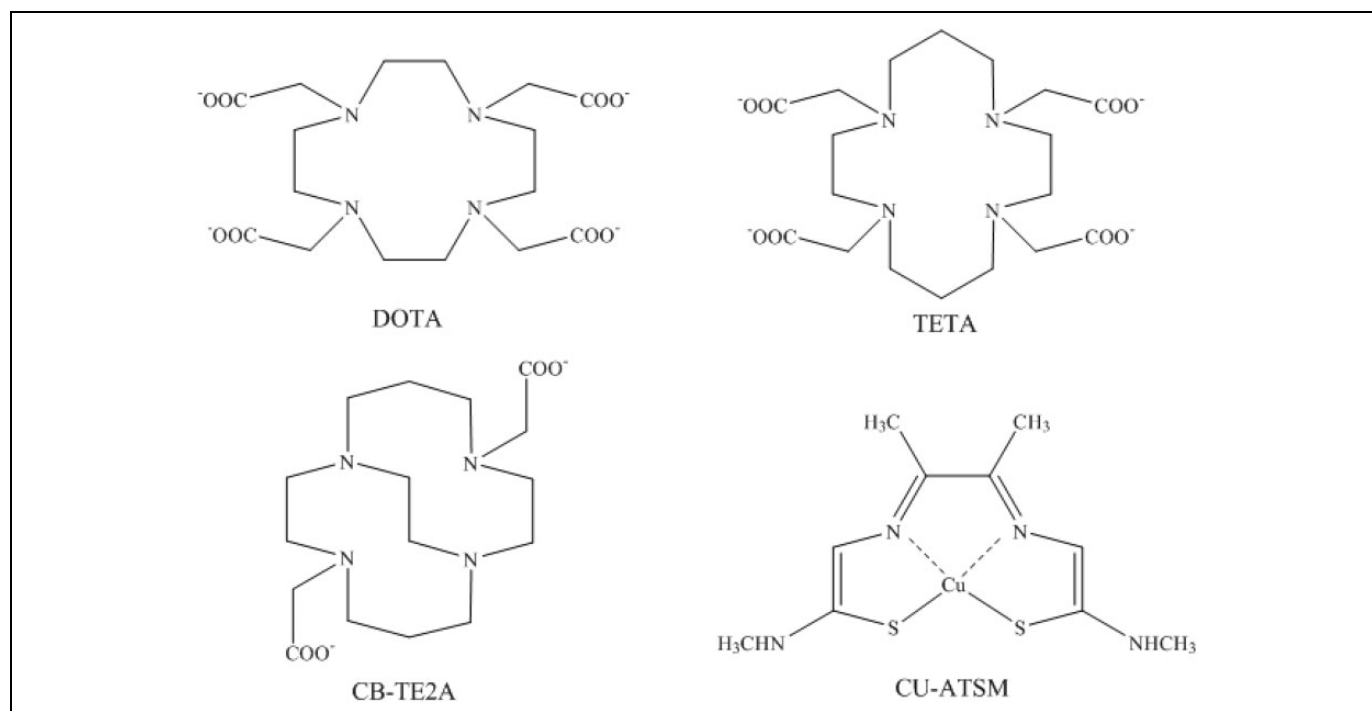Emails: dshming@163.com; wuyiwei3988@gmail.com

Figure 1. DOTA, CU-ATSM, CB-TE2A, and TETA the most common bifunctional chelators used for labeling biomolecules. DOTA indicates 1,4,7,10-tetraazacyclododecane-1,4,7,10-tetraacetic acid; ATSM, Diacetyl bis(N 4-methylthiosemicarbazone); CB-TE2A, 4,11-bis(carboxymethyl)-1,4,8,11-tetraazabicyclo[6.6.2]hexadecane; TE2A, 1,4,8,11-tetraazacyclotetradecane-1,8-diacetic acid.

Table 1. Decay Characteristics of Copper Radioisotopes.

Isotope	$T_{1/2}$	Decay Mode	Energy, Kev
^{60}Cu	23.7 min	β^+ (93%)	2940,3920
		γ (7%)	511-467-826-1332
^{61}Cu	3.3 h	β^+ (60%)	1220,1159
		γ (40%)	511-283-589-656
^{62}Cu	9.7 min	β^+ (98%)	2925
		γ (2%)	511
^{64}Cu	12.7 h	β^+ (19%)	657
		γ (43%)	511-1346
		β^- (38%)	141
^{67}Cu	62.0 h	β^- (100%)	390-482-575
		γ (52%)	91-93-185

Table 2. ^{64}Cu-Based Radiopharmaceuticals in Molecular Application.

Compound		Aim	Disease
^{64}Cu-ATSM		Imaging	Head and neck cancer,[15] lung cancer,[16] cervical cancer,[18,19] gliosarcoma[20]
		Therapy	Colon cancer[25]
^{64}CuCl$_2$		Imaging	Brain tumors,[30] prostate cancer[33]
^{64}Cu-antibodies	Trastuzumab	Imaging	Breast cancer[35]
		Therapy	Breast cancer[37]
	Cetuximab	Imaging	Targeting EGFR-expressing tumors[5]
	TRC105-Fab	Imaging	Breast cancer[45]
^{64}Cu-$\alpha_v\beta_3$-targeting antibodies		Imaging	Glioblastomas; breast cancer; prostate cancer; malignant melanomas; ovarian carcinomas[5]
^{64}Cu-somatostatin analogues		Imaging	Neuroendocrine tumors[57]
^{64}Cu-AE105		Imaging	Breast cancer,[65] lung cancer,[66] colorectal cancer,[67] prostate cancer,[68] bladder cancer[69]
^{64}Cu- PSMA - 617		Imaging	Prostate cancer[77]
^{64}Cu- DOTA-alendronate		Imaging	Breast cancer[82]

decade. A number of compounds coupled with Cu have been proposed not only for PET diagnostic imaging but also for targeted radiotherapy of tumor. Table 2 lists the most popular radiopharmaceuticals that were modified to be used with ^{64}Cu for cancer imaging and therapy. In the present study, we aimed to systematically review several commonly used biomarkers of ^{64}Cu radionuclide.

Production of Cu Radioisotope

The 2 potential ways to produce Cu radioisotopes include the use of the cyclotron or the reactor.[6] Copper-64, the most commonly used copper radionuclide, is characterized by a unique decay scheme (β^+: 19%, β^-: 38% and electron capture: 43%).

Such property allows either cyclotron or reactor production, and the latter route results in either low-specific activity (n, γ) or high-specific activity (n, p) products.[5]

Szelecsenyi *et al*[7] proposed ^{64}Cu reaction on a biomedical cyclotron, and small irradiations were performed to demonstrate the feasibility of ^{64}Cu production by this method. At present, the most common production method for ^{64}Cu utilizes the [64]Ni (p, n) ^{64}Cu reaction,[5] which yields a large quantity of nuclides with high-specific activity. However, such method needs enriched [64]Ni leading to increased overall costs.[8]

The target for producing ^{64}Cu is enriched [64]Ni (99.6%).[9] The [64]Ni is plated on the gold disk using a procedure modified from Piel *et al*.[10] At Washington University School of Medicine, ^{64}Cu is produced on a CS-15 cyclotron using 15.5 MeV protons (15-45 µA beam current) by the [64]Ni(p, n) ^{64}Cu reaction. After bombardment, the ^{64}Cu is separated from the target nickel in a 1-step procedure using an ion-exchange column.[9]

[64]Zn (n, p) ^{64}Cu reaction in nuclear reactor is another method for production of [64]Cu.[11] Most reactor-produced radionuclides are produced through thermal neutron reactions or (n, γ) reactions. Thermal neutrons have an advantage of relatively low cost, and its target material is of the same element as the product radionuclide. Meanwhile, in order to generate ^{64}Cu with a high specific activity, fast neutrons are employed to bombard the target in an (n, p) reaction. Unlike a thermal neutron reaction, a fast or highly energetic neutron has sufficient energy to eject a particle from the target nucleus.[12] However, many highly radioactive by-products of the reaction need to be removed and handled properly.[1]

[64]Cu-diacetyl-bis (N4-methylthiosemicarbazone)

Hypoxia is a pathological condition arising in living tissues when oxygen supply does not adequately cover the cellular metabolic demand. Tomlinson and Gray, for the first time, have demonstrated the presence of hypoxia in human tumors in the early 1960s,[13] and the hypoxic tissue in the tumors has certain resistance to traditional radiotherapy and chemotherapy, leading to increased aggressiveness, metastatic spread, enhanced rate of recurrence, and ultimately poor outcomes.[14] Therefore, an important relationship exists between the assessment of tumor hypoxia and prognosis. Hypoxic regions can be visualized by combination of PET and oxygen-dependent cellular uptake of radiopharmaceuticals. In recent years, Cu-diacetyl-bis (N4-methylthiosemicarbazone) (Cu-ATSM) labeled with a positron-emitting isotope of copper, such as [60]Cu, [62]Cu and ^{64}Cu, has been developed as an imaging agent targeting the hypoxic regions in tumors for use with PET.[15-20] Cu-ATSM has high membrane permeability and low redox potential, and it can passively diffuse within the intracellular environment to maintain the stability of normal tissue.

Mechanisms underlying the selective uptake of ^{64}Cu-ATSM in hypoxic areas still remain largely unexplored. Fujibayashi *et al*[21] suggested that Cu(II)-ATSM reduction occurs only in hypoxic cells due to the abnormally reduced state of their mitochondria and does not occur in normoxic cells. With extensive research on ^{64}Cu-ATSM, another mechanism is that Cu(II)-ATSM is reduced by thiols and converted into Cu(I)-ATSM complex both in normal and in hypoxic cells.[22] In normal cells, [64]Cu(I)-ATSM is again oxidized to [64]Cu(II)-ATSM and then freely diffused out of the cells.[23] Under hypoxic conditions, this complex is less stable than its bivalent form and progressively dissociated into H_2-ATSM and free Cu(I), which are then rapidly entrapped in intracellular proteins.[21]

McCall *et al*[15] assessed the role of ^{64}Cu-ATSM in head and neck squamous cell carcinoma (HNSCC) xenograft model through a combination of *in vivo* PET imaging and *in vitro* autoradiography and founded that the uptake of ^{64}Cu-ATSM in tumors was significantly higher than that in muscles. The PET image showed large tumor-to-muscle ratios, which were continually increased over an 18-hour period of imaging after injection. The results indicated that ^{64}Cu-ATSM uptake was specific for malignant expression. A prospective study[16] assessed the prognostic significance of ^{64}Cu-ATSM in 18 patients with locally advanced non-small cell lung cancer (NSCLC; n = 7) or head and neck cancer (HNC; n = 11) before treatment. Semi-quantitative and quantitative parameters on PET were calculated, including standardized uptake value $(SUV)_{max}$, $SUV_{ratio-to\ muscle}$, SUV_{mean}, hypoxic tumor volume (HTV), and hypoxic burden ($HB = HTV \times SUV_{mean}$). These data were subsequently correlated to disease outcomes, which were expressed in terms of progression-free survival calculated on a follow-up period with a median of 14.6 months. These analyses demonstrated that volumetric parameters were the most robust predictors of outcome, and patients with lower HTV and HB tend to have a better prognosis. Another prospective study[17] also assessed the prognostic role of ^{64}Cu-ATSM PET/CT pretreatment in 11 patients with HNC (III-IV). No significant difference was found in SUV_{max} between early (1 hour post injection) and late (16 hours post injection) acquisitions. Moreover, ^{64}Cu-ATSM showed high sensitivity (true positive rate, the percentage of positives that are correctly identified; 100%) but low specificity (true negative rate, the percentage of negatives that are correctly identified) in predicting therapy response based on both SUV_{max} and HTV, which can be probably attributed to the presence of undetectable hypoxia with the current method. Besides, 18F-fluorodeoxyglucose (^{18}F-FDG) and ^{64}Cu-ATSM provide similar results about delineation of biological tumor volume.

Several studies were conducted using [60]Cu in cervical cancer, and similar results in predicting the tumor response to therapy were obtained.[18] In fact, the pattern and magnitude of tumor uptake of [60]Cu and ^{64}Cu-ATSM are similar even if image quality is better in ^{64}Cu than in [60]Cu.[19] Therefore, ^{64}Cu-ATSM may be a predictive indicator of tumor response to therapy in patients with cervical cancer.

In 9 gliosarcoma rat models,[20] ^{64}Cu-ATSM uptake was measured in tumor tissue under different oxygen partial pressures (pO_2), and there was a good correlation between low pO_2 and high ^{64}Cu-ATSM accumulation. The uptake of ^{64}Cu-ATSM in tissues *in vivo* depends on the tissue pO_2, and significantly greater uptake and retention occur in hypoxic tumor tissue.

Since radiation resistance of hypoxic tumor is a well-known phenomenon, it is very important to assess the extent and location of hypoxia within a tumor. As a hypoxia imaging agent with high tumor-to-background ratios, ^{64}Cu-ATSM allows targeting of positive lesions with high sensitivity and specificity on PET. Hypoxia imaging-guided intensity-modulated radiation therapy can deliver higher dose of radiation to the hypoxic tumor and normal tissues.

However, some preclinical data suggested that ^{64}Cu-ATSM was not a hypoxia marker in all types of tumor. Vāvere et al[24] found that the relationship between ^{64}Cu-ATSM and overexpression of fatty acid synthase (FAS) was associated with prostate cancer (PCa), and the physiological significance of the FAS pathway in PCa was the harnessing of its oxidizing power for improving redox balance (ie, lower $NADH/NAD^+$ ratios), despite under oxygen-limiting (hypoxic) conditions causing low ^{64}Cu-ATSM uptake in hypoxic and normoxic regions. Therefore, the translation of ^{64}Cu-ATSM to imaging of PCa may be limited by the overexpression of FAS associated with prostatic malignancies.

[64]Cu is not only useful for PET imaging but also has potential as an agent for internal radiotherapy, since its favorable β^- decay (38%) and Auger electrons emitted from this nuclide can damage tumor cells.[25,26] Yukie et al[26] studied the therapeutic effect of ^{64}Cu-ATSM in HT-29 tumor-bearing mice after treating with bevacizumab, and the results showed that ^{64}Cu-ATSM effectively inhibited the growth of HT-29 tumors, exhibiting bevacizumab-induced vascular decrease and hypoxia. Therefore, it prolongs the survival of mice during bevacizumab treatment with negligible toxic side effects. Jason et al[25] also found that ^{64}Cu-ATSM significantly increased the survival time of hamsters bearing human GW39 colon cancer tumors. Yoshii et al[27] showed that the ^{64}Cu-ATSM uptake region of tumors was associated with upregulation of DNA repair and a high ratio of $CD133^+$ cells. $CD133^+$ cells have been reported to be highly resistant to conventional radiotherapy and chemotherapy in many types of cancer. ^{64}Cu-ATSM decreased the number of $CD133^+$ cells not via specific interactions, but it was accumulated in $CD133^+$ cell-rich regions within tumor, leading to higher doses of radiation in those areas.[28]

[64]CuCl$_2$

[64]CuCl$_2$, as the substrate of CTR1, has been demonstrated as a promising PET tracer for imaging animal models with tumors, such as melanoma, glioblastoma multiform, and PCa.[29-31] More importantly, some studies have shown that [64]CuCl$_2$-PET/CT is used in human study.[30,32] Peng et al[31] found that human PCa xenografts may be localized by PET using [64]CuCl$_2$ as a probe. Piccardo et al[33] prospectively evaluated 50 patients with PCa and showed that [64]CuCl$_2$ PET/CT possessed a significantly higher detection rate than ^{18}F-choline PET-CT. Jiang et al[34] studied animal models of H_2O_2-induced muscle inflammation and lipopolysaccharide-induced lung inflammation and revealed that the inflammatory muscles and lungs had a significantly higher ^{64}Cu accumulation than their corresponding

controls ($P < .05$). The potential diagnostic role of [64]CuCl$_2$ PET/CT imaging for brain malignancies has been recently evaluated in 19 patients with a documented history and radiologic evidence of cerebral tumors.[30] After initial cerebral magnetic resonance imaging (MRI), patients were administered with [64]CuCl$_2$ (13 MBq/kg), and brain PET/CT imaging was performed at 1, 3, and 24 hours after administration. Excellent agreement was found between PET/CT and MRI. Brain cancerous lesions can be clearly visualized within 1 hour after injection of [64]CuCl$_2$, with stable retention of radioactivity up to 24 hours. The radioactivity was cleared rapidly from the blood and mostly excreted through the liver. The major limitation of this study was that only a small number of patients were enrolled. However, these preliminary clinical data suggested that [64]CuCl$_2$ can be a potentially useful diagnostic agent for malignancies of the central nervous system (CNS).

[64]Cu-Labeled Antibodies for Tumor Targeting

As a large class of biotechnologically created proteins, monoclonal antibodies (mAbs) have been increasingly used in immunotherapy, targeted drug delivery, and *in vivo/in vitro* diagnostics. Trastuzumab (breast cancer expressing human epidermal growth factor receptor [EGFR] 2 or human epidermal growth factor receptor [HER2]), cetuximab (targeting EGFR-expressing tumors), TRC105-Fab (targeting CD105), and etaracizumab (antibody against human $\alpha_v\beta_3$ integrin) are the main monoclonal antibodies for ^{64}Cu labeling for PET imaging.[2]

[64]Cu-trastuzumab

HER2 status in breast cancer determines its therapeutic strategy.[35] Humanized anti-HER2 antibody trastuzumab is a well-established therapeutic strategy for HER2-positive breast cancer in neoadjuvant, adjuvant, and metastatic settings, and it increases overall survival for patients with HER2-positive breast cancer.[36] Several reports showed that ^{64}Cu-DOTA-trastuzumab PET imaging can be used to visualize primary and metastatic HER2-positive lesions[35-38] and better identify patients who may benefit from these expensive and potentially toxic treatments through a noninvasive approach.

Sasada et al[35] evaluated the concordance of HER2 expression in primary breast tumors between HER2-PET imaging and immunohistochemistry (IHC) in 38 patients with breast cancer. Significant difference in mean SUV_{max} value was found between HER2-positive and HER2-negative breast tumors, and SUV_{max} values were correlated with HER2-IHC scores (correlation coefficient = .619). When the cutoff value of SUV_{max} by HER2-PET imaging was set at 1.98, the sensitivity, specificity, and accuracy (the correctly identified fraction among the whole instances) were 83.3%, 88.2%, and 85.7%, respectively. Another study evaluated the feasibility and potential utility of ^{64}Cu-DOTA-trastuzumab PET/CT for lesion detection and uptake measurement in 6 patients with HER2-positive metastatic breast cancer.[37] After initial ^{18}F-FDG PET/CT, patients

were administered with 45 mg ^{64}Cu-DOTA-trastuzumab, and PET/CT imaging was performed 21 to 25 (day 1) and 47 to 49 (day 2) hours after injection of ^{64}Cu-DOTA-trastuzumab. The results showed that ^{64}Cu-DOTA-trastuzumab was rapidly accumulated in tumors after 1 hour of injection, and the detection sensitivity on day 1 and day 2 were 77% and 89%, respectively. Besides, no unanticipated toxicities or adverse side effects were observed in these 6 patients. The authors concluded that ^{64}Cu-DOTA-trastuzumab PET/CT was a practically and acceptably safe procedure in patients with metastatic breast cancer. A preliminary clinical study suggested that HER2-specific ^{64}Cu-DOTA-trastuzumab also accumulated in brain metastasis as evidenced by autoradiography, IHC, and liquid chromatography-tandem mass spectrometry.[38]

[64]Cu-cetuximab

EGFR is a member of the erbB family of tyrosine kinase receptors,[39] and the dysregulation of EGFR leads to several key features of cancer, such as autonomous cell growth, apoptosis and inhibition of angiogenesis, invasion, and metastases.[40] However, many studies have found that EGFR is overexpressed in many human tumors, including HNSCC, colon cancer, NSCLC, and cervical cancer.[41,42] Cetuximab with high affinity to EGFR, which was the first mAb against the EGFR or the treatment of patients with EGFR-expressing metastatic colorectal carcinoma approved by the US Food and Drug Administration.[5] In recent decades, radio-labeled anti-EGFR antibodies, such as ^{64}Cu-cetuximab, were studied for diagnosis, monitoring, and efficacy evaluation of EGFR-expressing tumors.

Cai *et al*,[42] for the first time, evaluated the quantitative PET imaging of EGFR expression in xenograft-bearing mice using ^{64}Cu-labeled cetuximab. In this study, 7 different types of cancer cell lines (U87MG human glioblastoma, PC-3 human prostate carcinoma, CT-26 murine colorectal carcinoma, HCT-8, HCT-116, and SW620 human colorectal carcinoma, and MDA-MB-435 human breast cancer) were selected, and a good correlation ($R^2 = .80$) between the tracer uptake (measured by PET) and the EGFR expression (measured by Western blotting) was confirmed. As expected, ^{64}Cu-DOTA-cetuximab showed significantly increased accumulation of tumor activity over time in EGFR-positive tumors (U87MG and PC-3 tumors), but it had relatively low uptake in EGFR-negative tumors (<5% ID/g). The radioactivity was mainly cleared through the hepatic pathway, and virtually no renal uptake or renal clearance was observed. The results of this study further revealed the potential utility of cetuximab for tumor diagnosis using PET as well as for determining patient-specific therapies and therapeutic efficacy monitoring.

In another interesting study, Laura *et al*[43] developed and characterized an EGFR-directed PET tracer, ^{64}Cu-cetuximab-F(ab′)2, to determine the systemic accessibility of EGFR. The authors selected male mice bearing human HNSCC xenografts UT-squamous cell carcinoma (SCC-8; n = 6) or UT-SCC-45 (n = 6). After 1 mouse for each tumor model was injected with excess unlabeled cetuximab (1 mg) for 3 days, ^{64}Cu-cetuximab-F(ab′)2 (21 ± 2.6 MBq,15 μg, 250 μL) PET/CT imaging was performed for UT-SCC-8and UT-SCC-45 mice. *In vivo* PET imaging and biodistribution studies demonstrated significant tumor uptake with good tumor-to-background signal at 24 hours after injection. The results indicated that ^{64}Cu-cetuximab-F(ab′)2 uptake was correlated with EGFR expression in both tumors, and UT-SCC-8 had a significantly higher expression of EGFR compared to UT-SCC-45. The preclinical data indicated the potential of ^{64}Cu-cetuximab-F(ab′)2 as a clinical EGFR-targeting tracer.

[64]Cu-TRC105-Fab

Tumor cells rely on newly formed tumor vessels for adequate nutrition during tumor growth, without which they cannot grow beyond a critical size or metastasize to another organ.[44] In the past 2 decades, efforts were made to find specific markers for newly formed tumor angiogenesis, and many targets have been widely studied for noninvasive imaging of tumor angiogenesis.[45,46] CD105 is mainly overexpressed on proliferating endothelial cells, and it is a promising candidate for tumor vascular targeting. High CD105 intratumor microvessel density is correlated with lower patient survival rates in multiple solid cancers, such as breast cancer, gastrointestinal, cancer, and PCa.[47]

As an accepted standard approach to identify actively proliferating tumor vessels, CD105 IHC has several potential advantages over the other targets, including overexpression in many solid malignancies, effective evaluation of the efficacy of antiangiogenic treatments, independence of its expression on neoplastic cells, lack of tumor histotype specificity, and immediate accessibility of malignant lesions through the blood stream.[5] With good affinity and specificity for CD105 on the tumor vasculature, radiolabeled TRC105-Fab can be potentially used as a promising imaging and diagnostic vascular agent for PET imaging in human tumors.[45]

Yin *et al*[45] reported PET imaging of CD105 expression in 4T1 murine model of breast cancer using [61/64]Cu-NOTA-TRC105-Fab, exhibiting prominent and target-specific uptake in the 4T1 tumor. Besides, the use of a Fab fragment leads to much faster tumor uptake (which peaks at a few hours after tracer injection) compared to radio-labeled intact antibody, which may be translated into same-day immune-PET imaging for clinical investigation.

[64]Cu-Integrin-Targeting Peptides

As a transmembrane glycoprotein receptor and an important cell adhesion molecule, alpha v beta 3 ($\alpha_v\beta_3$) plays important roles in tumor growth, invasion, metastasis, and angiogenesis.[48] It is highly expressed on various types of tumor cells, including glioblastomas, breast cancer, PCa, malignant melanomas, and ovarian carcinomas.[5] The cyclic pentapeptide containing a tripeptide sequence Arg-Gly-Asp (cRGD) has been identified with high specificity and affinity for the $\alpha_v\beta_3$.[48]

Sprague et al[49] evaluated ^{64}Cu-labeled c(RGDyK) peptides conjugated to a different chelator, CB-TE2A, and found that the corresponding ^{64}Cu complex was taken up specifically by osteoclasts, which were upregulated in osteolytic lesions and bone metastases. Ocak et al[50] compared ^{64}Cu-labeled c(RGDyK) peptides with previously reported CB-TE2A conjugates of c(RGDyK) for imaging osteoclasts in the 4T1 mouse, a mammary tumor model of bone metastases. This study demonstrated that although all chelator-peptide conjugates showed similar binding affinity for integrin $\alpha_v\beta_3$, the *in vivo* tumor targeting of CB-TE1A1P was superior to CB-TE2A-c(RGDyK). There is also improved kidney function and liver clearance for ^{64}Cu-TE1A1P-DBCO-c(RGDyK). In addition, PET imaging with ^{64}Cu-labeled c(RGDyK) can be informative for diagnosis and/or monitoring treatment for other diseases with high levels of osteoclasts, such asosteoarthritis.[51,52]

[64]Cu-Somatostatin Analogues

Somatostatin (SST) receptors (SSTRs) are G-protein-coupled receptors expressed on cell membranes, and 5 subtypes of SSTRs (SSTRl to SSTR5) have been identified to date.[53] The SSTRs are highly expressed in neuroendocrine tumors (NETs), such as pheochromocytoma, pituitary adenoma, carcinoid tumor, and medullary thyroid carcinoma, but they are also positive on the cell surfaces of other non-neurocytic tumor cells, including gliomas, meningioma, small cell lung cancer, and neuroblastoma.[54]

SST and its analogues bind to SSTRs with high affinity and high specificity, inactivate the signal transcription, and suppress the growth of corresponding tissue cells, thereby inhibiting the growth of tumor cells.[55] An 8-amino acid analog of SST, octreotide (OC), possesses a longer biologic half-life, and it is much more effective in inhibiting the secretion of growth hormone compared to SST.[14] Several radiotracers containing an SST analog chelated to a radioisotope were developed for SSTR imaging.

Anderson et al[56] demonstrated that ^{64}Cu-TETA-OC can be used to detect SSTR-positive tumors in humans. ^{64}Cu-TETA-OC PET shows higher rate of lesion detection, good sensitivity, favorable dosimetry, and pharmacokinetics for NET imaging compared to ^{111}In-DTPA-OC SPECT, partially due to the greater sensitivity of PET. Pfeifer et al[57] prospectively studied 112 patients with pathologically confirmed NETs of gastroenteropancreatic or pulmonary origin and found that the diagnostic sensitivity, accuracy, and negative predictive value (NPV; the fraction of correctly identified as negatives among the whole instances that were identified as negatives) of ^{64}Cu-DOTA-TATE were higher than those of ^{111}In-DTPA-OC (97%, 97%, and 80% vs 87%, 88%, and 48%, respectively). Results showed that the diagnostic value of ^{64}Cu-DOTA-TATE in patients with NETs was significantly better than that of ^{111}In-DTPA-OC. Therefore, ^{64}Cu-TETA-OC can replace ^{111}In-DTPA-OC in diagnosis of NETs. A similar head-to-head comparison was conducted to assess the diagnostic value

of ^{64}Cu-DOTA-TATE and ^{68}Ga-DOTA-TOC in 59 patients with NETs.[58] In the 68 inconsistent imaging areas, ^{64}Cu-DOTA-TATE showed 42 sites, of which 33 were found to be true positive (correctly identified instances) on follow-up. Moreover, 26 sites were detected by ^{68}Ga-DOTA-TOC, of which 7 were confirmed to be true-positive during follow-up. ^{64}Cu-DOTA-TATE finds an additional 83% of the true-positive sites, and the results showed that ^{64}Cu-DOTA-TATE had advantages over ^{68}Ga-DOTATOC in the detection of lesions in patients with NETs. In addition, ^{64}Cu-DOTA-TATE has a shelf life of more than 24 hours and a scanning window of at least 3 hours, making it advantageous and easy to use in a clinical setting.

Unfortunately, it was reported that Cu-TETA chelates were instable *in vivo*, since ^{64}Cu may dissociate from the TETA chelator and bind to proteins, primarily superoxide dismutase (SOD).[58] Using metabolism studies, Bass et al demonstrated that when ^{64}Cu-TETA-OC was injected into normal Sprague-Dawley rats, approximately 69% of the ^{64}Cu dissociates from ^{64}Cu-TETA-OC and binds to the protein SOD in the liver.[59] Clinical PET studies using ^{64}Cu-TETA-OC also resulted in retention of ^{64}Cu-TETA-OC in the blood and poor liver clearance in patients.[56] In another biodistribution study,[54] similar results were observed that ^{64}Cu-DOTA-TOC had a lower stability, showing slower blood clearance and high accumulation in the liver and intestine. Sun et al[60] evaluated the radiochemistry and biodistribution of 4 ^{64}Cu-labeled cross-bridged cyclam ligands and found that ^{64}Cu-CB-TE2A (CB-TC2A-4, 11-bis (carboxymethyl)-1, 4, 8, 11- tetraazabicycl[6.6.2] hexadecane) had the most rapid clearance through blood, liver, and kidney compared to ^{64}Cu-TETA. Sarkar et al[61] investigated the biophysical and chemical properties of 5 closely related bifunctional chelators and showed that significant differences in tissue uptake and clearance patterns were dependent on the chelator utilized in the peptide conjugate. Conjugates containing propylene cross-bridged chelators show higher tumor uptake and ultrahigh *in vivo* stability, while a closely related ethylene cross-bridged analogue exhibits rapid body clearance.

Malmberg et al,[62] for the first time, compared the large arterial uptake of ^{68}Ga-DOTA-TOC and ^{64}Cu-DOTA-TATE in 60 patients with NETs. The results showed that the uptake of ^{64}Cu-DOTA-TATE was significantly higher compared to ^{68}Ga-DOTA-TOC in the vascular regions. Besides, the uptake of ^{64}Cu-DOTA-TATE, but not ^{68}Ga-DOTA-TOC, was correlated with cardiovascular risk factors, suggesting a potential role for ^{64}Cu-DOTA-TATE in the assessment of atherosclerosis even in the subclinical stages.

[64]Cu-AE105

Extensive amount of studies implicated that the serine protease urokinase-type plasminogen activator (uPA) and its receptor (uPAR) were strongly prognostic in cancer invasion and metastasis.[63,64] In line with this finding, several studies reported that uPAR was associated with poor prognosis and metastatic disease in various tumors, such as breast,[65] lung,[66] colorectal,[67]

PCa,[68] and bladder[69] cancers. ^{64}Cu-DOTA-AE105 is a promising uPAR-PET ligand in several preclinical validation studies on PET imaging due to the high affinity of peptide antagonist AE105.[70]

The first in-human use of ^{64}Cu-DOTA-AE105 dates back to 2013, when Persson et al[71] evaluated the safety, pharmacokinetics, and dosimetry of a single-dose injection of ^{64}Cu-DOTA-AE105 in cancer patients by serial PET-CT imaging. ^{64}Cu-DOTA-AE105 was well tolerated, and no adverse or clinically detectable side effects were found. The effective radiation dose was found to be 0.0276 mSv/MBq, and the liver was the organ with the highest absorption, followed by kidneys. In addition, high uptake in both primary tumor lesions and lymph node (LN) metastases were seen and paralleled by high uPAR expression in excised tumor tissue. The study concluded that uPAR-PET imaging seemed to be a highly promising technology with strong prognostic factor in patients with cancer. However, large controlled clinical trials have further indicated that these results are highly necessary.

[64]Cu-Prostate-Specific Membrane Antigen Ligand 617

Prostate-specific membrane antigen (PSMA) is a unique cell membrane surface protein,[72] which is overexpressed in PCa cells, particularly in advanced and metastatic disease, but its expression is limited in normal tissues. Low-molecular-weight radioligands have a relatively short cycle time and can be rapidly cleared from the target tissues.[73] Recently, 2-[3-(1-carboxy-5-{3-naphthalen-2-yl-2-[(4-{[2-(4,7,10-tris-carboxymethyl-1,4,7,10- tetraazacyclododec-1-yl) acetylamino]methyl} cyclohexanecarbonyl) amino] propionylamino} pentyl) ureido]-pentanedioic acid (PSMA-617) has been developed as a novel PSMA ligand. ^{68}Ga-PSMA PET/CT has a higher sensitivity than other radionuclides (^{18}F) in the detection of PCa.[74] However, due to the short half-life of ^{68}Ga, its application is limited to clinical PET centers with radiochemistry facility and a ^{68}Ga generator available on site, and a limited accuracy is found in detecting small lesions and LNs with diameters <6 mm.[75] Recently, studies were conducted using the ^{64}Cu alternative ^{68}Ga label PSMA. Radionuclides with a longer half-life, such as [64]Cu ($T_{1/2}$ = 12.7 hours), allow sufficient time to clear nonspecific radioactivity in the background tissue, resulting in high tumor-to-organ ratios.[76] In addition, ^{64}Cu emits lower positron energy than ^{68}Ga, and therefore it has better image resolution.

The first in-human use of ^{64}Cu-labeled ligand PSMA-617 for PET imaging in PCa occurs at 2 different centers in Austria and Germany.[77] In this study, the advantages of a small PSMA-targeting agent and a long-lived positron emitter with good image quality were combined, and ^{64}Cu-PSMA-617 resulted in high image contrast. All cases with histologically proven local diseases (23 of 29 patients) were clearly identified by ^{64}Cu-PSMA-617 PET. Lesions suspicious for PCa were detected with excellent contrast as early as 1 hour post-injection, with high detection rates even at low prostate-specific antigen (PSA) levels. This study showed that ^{64}Cu-PSMA-617 PET/CT imaging had a high potential in the detection of PCa. Cantiello et al[78] assessed the diagnostic accuracy of ^{64}Cu-PSMA-617 PET/CT in the primary LN staging of 23 patients with intermediate- to high-risk PCa. The final pathological results were used as reference standards. The results displayed that ^{64}Cu-PSMA PET/CT was always positive on PCa, and SUV_{max} at 4 hours were significantly increased compared to that at 5 minutes and 1 hour in PCa and in LN metastases. The sensitivity, specificity, PPV (positive predictive value, the fraction of correctly identified as positives among the whole instances that were identified as positives), and NPV for LN staging of ^{64}Cu-PSMA PET/CT at 4 hours were 87.5%, 100%, 100%, and 93.7%, respectively. The receiver operating characteristic (ROC) curve showed the accuracy of ^{64}Cu-PSMA PET/CT in LN staging was characterized by an area under the curve of 0.938. In addition, there was a positive correlation between the 4-hour SUV_{max} and Gleason score, index, and cumulative tumor volume. These preliminary studies indicated that ^{64}Cu-PSMA-617 PET/CT had high potential in the diagnosis and LN staging of patients with PCa, but further extensive clinical studies are still needed.

[64]Cu-PSMA-617 is a novel radiotracer for tumor imaging not only in PCa but also expressed in many solid tumor angiogenic systems, such as gastric cancer and colon cancer.[79] The specificity of ^{64}Cu-PSMA-617 is confirmed by cell uptake experiments in PSMA(+) LNCaP cells as well as PSMA(−) PC-3 and gastric adenocarcinoma BGC-823 cells.[80]

Other Applications

In the past period of time, nanodevices and nanoparticles were used in biomedical research to investigate improved diagnostic and therapeutic agents.[14] When nanoparticles are linked to tumor targeting ligands, such as antibodies, proteins, peptides, or other biologically relevant small molecules, they can be used to target tumor antigens (biomarkers) as well as tumor vasculatures with high affinity and specificity.[81]

The studies assessed the use of ^{64}Cu-labeled DOTA-alendronate for PET imaging in normal or tumor-bearing aged, female, retired breeder Sprague-Dawley rats.[82] PET images showed excellent contrast between mammary microcalcifications and surrounding soft tissues. The study indicated that different types of tumors had significantly different ^{64}Cu-DOTA-alendronate uptakes, the radioactivity uptake in malignant tumors was higher than that in benign and normal tissues, and these variations in uptake (and resultant PET image intensity) were inversely proportional to the radiopacity of these tumor types on traditional mammograms. At the same time, the dosimetric analysis demonstrated a ^{64}Cu effective dose within the acceptable range for clinical PET imaging agents and the potential for translation into patients.

Conclusions

[64]Cu has an intermediate half-life of 12.7 hours and unique decay profile, making it a favorable option for radiolabeling

peptides, small molecules, and large biomolecules, such as antibodies and nanoparticles for PET imaging and radionuclide therapy. The versatility of copper and its compounds makes it a powerful advantage in the development of new pharmaceuticals. This is conducive to the greater role of nuclear medicine imaging in the diagnosis and treatment of diseases and will have a profound impact on the formation of new medical models and human health. However, studies reported that ^{64}Cu-TATE/^{64}Cu-DOTA was instable *in vivo*, and ^{64}Cu may dissociate from the TETA or DOTA chelator. Therefore, significant research has been devoted to the development of ligands that can stably chelate ^{64}Cu.

Authors' Note

Yeye Zhou and Jihui Li contributed equally to this work.

Declaration of Conflicting Interests

The author(s) declared no potential conflicts of interest with respect to the research, authorship, and/or publication of this article.

Funding

ORCID iD

Yeye Zhou, MB https://orcid.org/0000-0001-9797-3121

References

1. Wadas TJ, Wong EH, Weisman GR, Anderson CJ. Copper chelation chemistry and its role in copper radiopharmaceuticals. *Curr Pharm Des*. 2007;13(1):3-16.

2. Szymański P, Frączek T, Markowicz M, Mikiciuk-Olasik E. Development of copper based drugs, radiopharmaceuticals and medical materials. *Biometals*. 2012;25(6):1089-1112.

3. Ma W, Fu F, Zhu J, et al. ^{64}Cu-Labeled multifunctional dendrimers for targeted tumor PET imaging. *Nanoscale*. 2018;10(13): 6113-6124.

4. Follacchio GA, De Feo MS, De Vincentis G, Monteleone F, Liberatore M. Radiopharmaceuticals labelled with copper radionuclides: clinical results in human beings. *Curr Radiopharm*. 2018;11(1):22-33.

5. Niccoli Asabella A, Cascini GL, Altini C, Paparella D, Notaristefano A, Rubini G. The copper radioisotopes: a systematic review with special interest to ^{64}Cu. *Biomed Res Int*. 2014; 2014:786463. doi:10.1155/2014/786463.

6. Chakravarty R, Chakraborty S, Dash A. ^{64}Cu2+ Ions as PET Probe: an emerging paradigm in molecular imaging of cancer. *Mol Pharm*. 2016;13(11):3601-3612. doi:10. 1021/acs. Molpharmaceut.6b00528.

7. Szelecsenyi F, Blessing G, Qaim SM. Excitation function of proton induced nuclear reactions on enriched ^{61}Ni and ^{64}Ni:

8. Karimi Z, Sadeghi M, Matajikojouri N. ^{64}Cu, a powerful positron emitter for immunoimaging and theranostic: production via ZnO and ZnO-NPs. *Appl Radiat Isot*. 2018;137:56-61. doi:10.1016/j.apradiso.2018.03.007.

9. McCarthy DW, Shefer RE, Klinkowstein RE, et al. Efficient production of high specific activity ^{64}Cu using a biomedical cyclotron. *Nucl Med Biol*. 1997;24(1):35-43.

10. Piel H, Qaim SM, Stocklin G. Excitation functions of (p, xn)-reactions on nat Ni and highly enriched ^{62}Ni: possibility of production of medically important radioisotope 62 Cu on a small cyclotron. *Radiochimica Acta*. 1992;57:1-5.

11. Shokeen M, Anderson CJ. Molecular imaging of cancer with copper-64 radiophar rmaceuticals and positron emission tomography (PET). *Acc Chem Res*. 2009;42(7):832-841.

12. Zinn KR, Chaudhuri TR, Cheng TP, Morris JS, Meyer WA Jr. Production of no-carrier-added ^{64}Cu from zinc metal irradiated under boron shielding. *Cancer*. 1994;73(suppl 3):774-778.

13. Colombié M, Gouard S, Frindel M, et al. Focus on the controversial aspects of ^{64}Cu-ATSM in tumoral hypoxia mapping by PET imaging. *Front Med (Lausanne)*. 2015;2:58.

14. Anderson CJ, Ferdani R. Copper-64 radiopharmaceuticals for PET imaging of cancer: advances in preclinical and clinical research. *Cancer Biother Radiopharm*. 2009;24(4): 379-393.

15. Mccall KC, Humm JL, Bartlett R, Reese M, Carlin S. Copper-64-diacetyl-bis (N(4)- methylthiosemicarbazone) pharmacokinetics in FaDu xenograft tumors and correlation with microscopic markers of hypoxia. *Int J Radiat Oncol Biol Phys*. 2012;84(3):e393-e399. doi:10.1016/j.ijrobp.2012.0 5. 005.

16. Lopci E, Grassi I, Rubello D, et al. Prognostic evaluation of disease outcome in solid tumors investigated with ^{64}Cu-ATSM PET/CT. *Clin Nucl Med*. 2016;41(2):e87-e92. doi:10.1097/RLU. 0000000000001017.

17. Grassi I, Nanni C, Cicoria G, et al. Usefulness of ^{64}Cu-ATSM in head and neck cancer: a preliminary prospective study. *Clin Nucl Med*. 2014;39(1):e59-e63.

18. Grigsby PW, Malyapa RS, Higashikubo R, et al. Comparison of molecular markers of hypoxia and imaging with (60) Cu-ATSM in cancer of the uterine cervix. *MolImaging Biol*. 2007;9(5): 278-283.

19. Lewis JS, Laforest R, Dehdashti F, Grigsby PW, Welch MJ, Siegel BA. An imaging comparison of ^{64}Cu-ATSM and 60Cu-ATSM in cancer of the uterine cervix. *J Nucl Med*. 2008;49(7): 1177-1182.

20. Lewis JS, Sharp TL, Laforest R, Fujibayashi Y, Welch MJ. Tumor uptake of copper-diacetyl-bis(N(4)-methylthiosemicarbazone): effect of changes in tissue oxygenation. *J Nucl Med*. 2001; 42(4):655-661.

21. Fujibayashi Y, Taniuchi H, Yonekura Y, Ohtani H, Konishi J, Yokoyama A. Copper-62-ATSM: a new hypoxia imaging agent with high membrane permeability and low redox potential. *J Nucl Med*. 1997;38(7):1155-1160.

22. Chen K, Chen X. Positron emission tomography imaging of cancer biology: current status and future prospects. *Semin Oncol*. 2011;38(1):70-86.

23. Lopci E, Grassi I, Chiti A, et al. PET radiopharmaceuticals for imaging of tumor hypoxia: a review of the evidence. *Am J Nucl Med Mol Imaging*. 2014;4(4):365-384.

24. Vāvere AL, Lewis JS. Examining the relationship between Cu-ATSM hypoxia selectivity and fatty acid synthase expression in human prostate cancer cell lines. *Nucl Med Biol*. 2008;35(3):273-279. doi:10.1016/j.nucmedbio.2007.11. 012.

25. Lewis J, Laforest R, Buettner T, et al. Copper-64- Diacetyl-Bis(N4-Methylthiosemicarbazone): an agent for radiotherapy. *Proc Natl Acad Sci U S A*. 2001;98(3):1206-1211. doi:10.1073/pn as.98.3.1206.

26. Yoshii Y, Yoshimoto M, Matsumoto H, et al. ^{64}Cu-ATSM internal radiotherapy to treat tumors with bevacizumab-induced vascular decrease and hypoxia in human colon carcinoma xenografts. *Oncotarget*. 2017;8(51):88815-88826.

27. Yoshii Y, Furukawa T, Matsumoto H, et al. (64)Cu-ATSM therapy targets regions with activated DNA repair and enrichment of CD133 (+) cells in an HT-29 tumor model: sensitization with a nucleic acid antimetabolite. *Cancer Lett*. 2016;376(1):74-82.

28. Yoshii Y, Furukawa T, Kiyono Y, et al. Internal radiotherapy with copper-64-diacetyl-bis(N4 - methylthiosemicarbazone) reduces CD133+ highly tumorigenic cells and metastatic ability of mouse colon carcinoma. *Nucl Med Biol*. 2011;38(2):151-157.

29. Qin C, Liu H, Chen K, et al. Theranostics of malignant melanoma with [64]CuCl2. *J Nucl Med*. 2014;55(5):812-817.

30. Panichelli P, Villano C, Cistaro A, et al. Imaging of brain tumors with Copper-64 Chloride: early experience and results. *Cancer Biother Radiopharm*. 2016;31(5):159-167. doi:10.1089/cbr.2016.2028.

31. Peng F, Lu X, Janisse J, Muzik O, Shields AF. PET of human prostate cancer xenografts in mice with increased uptake of [64]CuCl$_2$. *J Nucl Med*. 2006;47(10):1649-1652.

32. Avila-Rodriguez MA, Rios C, Carrasco-Hernandez J, et al. Biodistribution and radiation dosimetry of [64]Cu.copper dichloride: first-in- human study in healthy volunteers. *EJNMMI Res*. 2017;7(1):98.

33. Piccardo A, Paparo F, Puntoni M, et al. [64]CuCl PET/CT in prostate cancer relapse. *J Nucl Med*. 2018;59(3):444-451.

34. Jiang L, Song D, Chen H, Zhang A, Wang H, Cheng Z. Pilot Study of [64]CuCl$_2$ for PET Imaging of Inflammation. *Molecules*. 2018;23(2):E502. doi:10.3390/molecules230 20502.

35. Sasada S, Kurihara H, Kinoshita T, et al. ^{64}Cu-DOTA-Trastuzumab PET imaging forHER2-specific primary lesions of breast cancer. *Ann Oncol*. 2017;28(8):2028-2029. doi:10.1093/annonc/mdx227.

36. Mortimer JE, Bading JR, Park JM, et al. Tumor Uptake of ^{64}Cu-DOTA-trastuzumab in patients with metastatic breast cancer. *J Nucl Med*. 2018;59(1):38-43. doi:10. 2967 /jnumed.117. 193888.

37. Mortimer JE, Bading JR, Colcher DM, et al. Functional imaging of human epidermal growth factor receptor 2-positive metastatic breast cancer using (64) Cu-DOTA-trastuzumab PET. *J Nucl Med*. 2014;55(1):23-29. doi:10.2967/jnumed.113.122630.

38. Kurihara H, Hamada A, Yoshida M, et al. ^{64}Cu-DOTA-trastuzumab PET imaging and HER2 specificity of brain metastases in HER2-positive breast cancer patients. *EJNMMI Res*. 2015;5:8. doi:10.1186/s13550-0 15-0082-6.

39. Arteaga C. Targeting HER1/EGFR: a molecular approach to cancer therapy. *Semin Oncol*. 2003;30(3 suppl 7):3-14.

40. Ping Li W, Meyer LA, Capretto DA, Sherman CD, Anderson CJ. Receptor-binding, biodistribution, and metabolism studies of [64]Cu- DOTA-cetuximab, a PET-imaging agent for epidermal growth-factor receptor-positive tumors. *Cancer Biother Radiopharm*. 2008;23(2):158-171. doi:10.1089/cbr.2007.0444.

41. Eiblmaier M, Meyer LA, Watson MA, Fracasso PM, Pike LJ, Anderson CJ. Correlating EGFR expression with receptor-binding properties and internalization of ^{64}Cu-DOTA-cetuximab in 5 cervical cancer cell lines. *J Nucl Med*. 2008;49(9):1472-1479.

42. Cai W, Chen K, He L, et al. Quantitative PET of EGFR expression in xenograft-bearing mice using ^{64}Cu-labeled cetuximab, a chimeric anti-EGFR monoclonal antibody. *Eur J Nucl Med Mol Imaging*. 2007;34(6):850-858. doi:10.1007/s00259-006 -0361-6.

43. van Dijk LK, Yim CB, Franssen GM, et al. PET of EGFR with (64) Cu-cetuximab-F(ab')2 in mice with head and neck squamous cell carcinoma xenografts. *Contrast Media Mol Imaging*. 2016;11(1):65-70. doi:10.1002/cmmi. 1659.

44. Carmeliet P, Jain RK. Angiogenesis in cancer and other diseases. *Nature*. 2000;407(6801):249-257.

45. Zhang Y, Hong H, Orbay H, et al. PET imaging of CD105 / endoglin expression with a [61 / 64] Cu-labeled Fab antibody fragment. *Eur J Nucl Med Mol Imaging*. 2013;40(5):759-767.

46. Zhang Y, Yang Y, Hong H, Cai W. Multimodality molecular imaging of CD105 (Endoglin) expression. *Int J Clin Exp Med*. 2011;4(1):32-42.

47. Dallas NA, Samuel S, Xia L, et al. Endoglin (CD105): a marker of tumor vasculature and potentialtarget for therapy. *Clin Cancer Res*. 2008;14(7):1931-1937.

48. Jin ZH, Furukawa T, Degardin M, et al. αvβ3 integrin-targeted radionuclide therapy with ^{64}Cu-cyclam-RAFT-c(-RGDfK-)4. *Mol Cancer Ther*. 2016;15(9):2076-2085.

49. Sprague JE, Kitaura H, Zou W, et al. Noninvasive imaging of osteoclasts in parathyroid hormone–induced osteolysis using a ^{64}Cu-Labeled RGD Peptide. *J Nucl Med*. 2007;48(2):311-318.

50. Ocak M, Beaino W, White A, Zeng D, Cai Z, Anderson CJ. Cu-labeled phosphonate cross-bridged chelator conjugates of c(RGDyK) for PET/CT imaging of osteolytic bone metastases. *Cancer Biother Radiopharm*. 2018;33(2):74-83.

51. Sambrook P, Cooper C. Osteoporosis. *Lancet*. 2006;367(9527):2010-2018.

52. Nakamura I, Duong LT, Rodan SB, Rodan GA. Involvement of alpha (v) beta3 integrins in osteoclast function. *J Bone Miner Metab*. 2007;25(6):337-344.

53. Patel YC. Somatostatin and its receptor family. *Front Neuroendocrinol*. 1999;20(3):157-198.

54. Hanaoka H, Tominaga H, Yamada K, et al. Evaluation of (64) Cu-labeled DOTA-D-Phe(1)–Tyr(3)-octreotide ((64)Cu-DOTA-TOC) for imaging somatostatin receptor-expressing tumors. *Ann Nucl Med*. 2009;23(6):559-567. doi:10.1007/s12149-009-0274-0.

55. Anderson CJ, Jones LA, Bass LA, et al. Radiotherapy, toxicity and dosimetry of copper-64-TETA-octreotide in tumor-bearing rats. *J Nucl Med*. 1998;39(11):1944-1951.

56. Anderson CJ, Dehdashti F, Cutler PD, et al. ^{64}Cu-TETA-octreotide as a PET imaging agent for patients with neuroendocrine tumors. *J Nucl Med*. 2001;42(2):213-221.

57. Pfeifer A, Knigge U, Binderup T, et al. ^{64}Cu-DOTATATE PET for neuroendocrine tumors: a prospective head-to-head comparison with 111In-DTPA- Octreotide in 112 Patients. *J Nucl Med*. 2015;56(6):847-854.

58. Johnbeck CB, Knigge U, Loft A, et al. Head-to-head comparison of ^{64}Cu-DOTATATE and ^{68}Ga-DOTATOC PET/CT: a prospective study of 59 patients with neuroendocrine tumors. *J Nucl Med*. 2017;58(3):451-457. doi:10.2967/jnumed.116.180430.

59. Bass LA, Wang M, Welch MJ, Anderson CJ. *In vivo* transchelation of copper-64 from TETA-octreotide to superoxidedismutase in rat liver. *Bioconjug Chem*. 2000;11(4):527-532.

60. Sun X, Wuest M, Weisman GR, et al. Radiolabeling and *in vivo* behavior of copper-64-labeled cross-bridged cyclam ligands. *J Med Chem*. 2002;45(2):469-477.

61. Sarkar S, Bhatt N, Ha YS, et al. High *in Vivo* Stability of ^{64}Cu-labeled cross-bridged chelators is a crucial factor in improved tumor imaging of RGD peptide conjugates. *J Med Chem*. 2018; 61(1):385-395. doi:10.1021/acs.jmedch em.7b01671.

62. Malmberg C, Ripa RS, Johnbeck CB, et al. ^{64}Cu-DOTATATE for noninvasive assessment of atherosclerosis in large arteries and its correlation with risk factors: head-to-head comparison with ^{68}Ga-DOTATOC in 60 Patients. *J Nucl Med*. 2015;56(12): 1895-1900. doi:10. 2967 /jnumed.115.161216.

63. Persson M, Kjaer A. Urokinase-type plasminogen activator receptor (uPAR) as a promising new imaging target: potential clinical applications. *Clin Physiol FunctImaging*. 2013;33(5):329-337.

64. Dass K, Ahmad A, Azmi AS, Sarkar SH, Sarkar FH. Evolving role of uPA / uPAR system in human cancers. *Cancer Treat Rev*. 2008;34(2):122-136.

65. Riisbro R, Christensen IJ, Piironen T, et al. Prognostic significance of soluble urokinase plasminogen activator receptor in serum and cytosol of tumor tissue from patients with primary breast cancer. *Clin Cancer Res*. 2002;8(5):1132-1141.

66. Pappot H, Høyer-Hansen G, Rønne E, et al. Elevated plasma levels of urokinase plasminogen activator receptor in non-small cell lung cancer patients. *Eur J Cancer*. 1997;33(6):867-872.

67. Pyke C, Ralfkiaer E, Rønne E, Høyer-Hansen G, Kirkeby L, Danø K. Immunohistochemical detection of the receptor for urokinase plasminogen activator in human colon cancer. *Histopathology*. 1994;24(2):131-138.

68. Akudugu J, Serafin A, Böhm L. Further evaluation of uPA and PAI-1 as biomarkers for prostatic diseases. *J Cancer Res Clin Oncol*. 2015;141(4):627-631.

69. Dohn LH, Illemann M, Høyer-Hansen G, et al. Urokinase-type plasminogen activator receptor (uPAR) expression is associated with T-stage and survival in urothelial carcinoma of the bladder. *Urol Oncol*. 2015;33(4):165.e15-e24.

70. Persson M, El Ali HH, Binderup T, et al. Dosimetry of ^{64}Cu-DOTA-AE105, a PET tracer for uPAR imaging. *Nucl Med Biol*. 2014;41(3):290-295.

71. Persson M, Skovgaard D, Brandt-Larsen M, et al. First-in-human uPAR PET: imaging of cancer aggressiveness. *Theranostics*. 2015;5(12):1303-1316.

72. Ghosh A, Heston WD. Tumor target prostate specific membrane antigen (PSMA) and its regulation in prostate cancer. *J Cell Biochem*. 2004;91(3):528-539. doi:10.1002/jcb.10661.

73. Cui C, Hanyu M, Hatori A, et al. Synthesis and evaluation of (64) Cu. PSMA-617 targeted for prostate-specific membrane antigen in prostate cancer. *Am J Nucl Med Mol Imaging*. 2017;7(2):40-52.

74. Afshar-Oromieh A, Zechmann CM, Malcher A, et al. Comparison of PET imaging with a ^{68}Ga-labelled PSMA ligand and 18 F-choline-based PET/CT for the diagnosis of recurrent prostate cancer. *Eur J Nucl Med MolImaging*. 2014;41(1):11-20.

75. Budäus L, Leyh-Bannurah SR, Salomon G, et al. Initial experience of (68)Ga-PSMA PET/CT imaging in high-risk prostate cancer patients prior to radical prostatectomy. *Eur Urol*. 2016; 69(3):393-396. doi:10.1016/j.eururo.2015.06.010.

76. Banerjee SR, Pullambhatla M, Foss CA, et al. 64 Cu-labeled inhibitors of prostate-specific membrane antigen for PET imaging of prostate cancer. *J Med Chem*. 2014;57(6):2657-2669.

77. Grubmüller B, Baum RP, Capasso E, et al. (64)Cu-PSMA-617 PET/CT imaging of prostate adenocarcinoma: first in-human studies. *Cancer Biother Radiopharm*. 2016;31(8):cbr.2015.1964.

78. Cantiello F, Gangemi V, Cascini GL, et al. Diagnostic accuracy of (64)Copper prostate-specific membrane antigen positron emission tomography/computed tomography for primary lymph node staging of intermediate-to high-risk prostate cancer: our preliminary experience. *Urology*. 2017;106:139-145. doi:10.1016/j.urology.2017.04.019.

79. Haffner MC, Kronberger IE, Ross JS, et al. Prostate-specific membrane antigen expression in the neovasculature of gastric and colorectal cancers. *Hum Pathol*. 2009;40(12):1754-1761. doi:10.1016/j.humpath.2009.06.003.

80. Han XD, Liu C, Liu F, et al. ^{64}Cu-PSMA-617: a novel PSMA-targeted radio-tracer for PET imaging in gastric adenocarcinoma xenografted mice model. *Oncotarget*. 2017;8(43):74159-74169.

81. Jain KK. Recent advances in nanooncology. *Technol Cancer Res Treat*. 2008;7(1):1-13.

82. Ahrens BJ, Li L, Ciminera AK, et al. Diagnostic PET imaging of mammary microcalcifications using (64) Cu-DOTA-alendronate in a rat model of breast cancer. *J Nucl Med*. 2017;58(9): 1373-1379.